Aerodynamic Aspects of Wind Energy Conversion

Jens Nørkær Sørensen

Department of Mechanical Engineering, Technical University of Denmark, DK-2800 Kongens Lyngby, Denmark; email: jns@mek.dtu.dk

Annu. Rev. Fluid Mech. 2011. 43:427–48

First published online as a Review in Advance on September 14, 2010

The *Annual Review of Fluid Mechanics* is online at fluid.annualreviews.org

This article's doi:
10.1146/annurev-fluid-122109-160801

0066-4189/11/0115-0427$20.00

Keywords

wind turbines, rotor aerodynamics, BEM theory, CFD, wakes, wind farms

Abstract

This article reviews the most important aerodynamic research topics in the field of wind energy. Wind turbine aerodynamics concerns the modeling and prediction of aerodynamic forces, such as performance predictions of wind farms, and the design of specific parts of wind turbines, such as rotor-blade geometry. The basics of the blade-element momentum theory are presented along with guidelines for the construction of airfoil data. Various theories for aerodynamically optimum rotors are discussed, and recent results on classical models are presented. State-of-the-art advanced numerical simulation tools for wind turbine rotors and wakes are reviewed, including rotor predictions as well as models for simulating wind turbine wakes and flows in wind farms.

1. BRIEF HISTORICAL REVIEW

Windmills have existed for more than 3,000 years and have greatly facilitated agricultural development. Even today when other types of machinery have taken over the windmills' jobs, the new machines are often called mills. Except for the propulsion of sailing ships, the windmill is the oldest device for exploiting the energy of the wind. Since the appearance of the ancient Persian vertical-axis windmills 3,000 years ago, many different types of windmills have been invented. In western Europe, the Dutch horizontal-axis windmill was for centuries the most popular type and formed the basis for the development of the modern wind turbine in the twentieth century. (The term windmill refers to a machine intended for grinding grain and similar jobs, whereas the term wind turbine refers to an electricity-producing machine.)

The first electricity-producing wind turbine was constructed by Charles F. Brush in the United States in 1887. Brush's machine had a 17-m-diameter rotor, consisting of 144 blades, and a 12-kW generator. In the period 1891–1908, unaware of the work of Brush, Poul La Cour undertook basic wind turbine research in Denmark. Based on his ideas, the design of aerodynamically efficient rotor blades soon advanced, and in 1918 approximately 3% of the Danish electricity consumption was covered by wind turbines. Whereas the first wind turbines used primitive airfoil shapes and produced electricity through a dynamo located in the tower, a new generation of wind turbines was developed in the mid-1920s that used modified airplane propellers to drive direct-current generators installed in the nacelle. One example is the Jacobs wind turbine developed by Jacobs Wind Electric Company, which, from the early 1930s, found widespread use in the United States in providing lighting for farms and charging batteries. However, in the following period fuel-based power became cheap and forced wind power out of the market.

Because of supply crises, renewed interest was paid to wind energy during World War II. This led to the construction of the American 1.25-MW Smith-Putnam machine, installed in Vermont in 1941, and the Danish F.L. Smith turbines built in 1941–1942. With a concept based on an upwind rotor with stall regulation and the use of modern airfoils, the F.L. Smith turbines can be considered as the forerunners of modern wind turbines. After World War II, the design philosophy of the F.L. Smith turbine was developed further, resulting in the Gedser turbine, which was constructed in 1957 (**Figure 1**). At the same time in Germany Ulrich Hütter developed a new approach comprising two fiberglass blades mounted downwind on a teetering hub. These turbines later became prototypes for the new generation of wind turbines put into production after the oil crisis in 1973. In the mid-1970s, many countries (e.g., United States, Germany, Great Britain, Sweden, the Netherlands, and Denmark) launched national programs to investigate the potential of producing electricity from the wind and carried out big demonstration projects. Together with the effort of a large number of small industries, this formed the basis for what is today an industry with a global annual turnover of more than 50 billion USD and an annual average growth rate of more than 20%. Today, state-of-the-art wind turbines have rotor diameters of up to 120 m and 5-MW installed power, and these are often placed in large wind farms with a production size corresponding to a nuclear power plant.

Although research in wind energy has taken place for more than a century now, there is no doubt that wind-energy competitiveness can be improved through further cost reductions, collaboration with complementary technologies, and new innovative aerodynamic design.

2. AERODYNAMIC RESEARCH IN WIND ENERGY

The aerodynamics of wind turbines concerns the modeling and prediction of the aerodynamic forces on solid structures and rotor blades of wind turbines. Aerodynamics is normally integrated

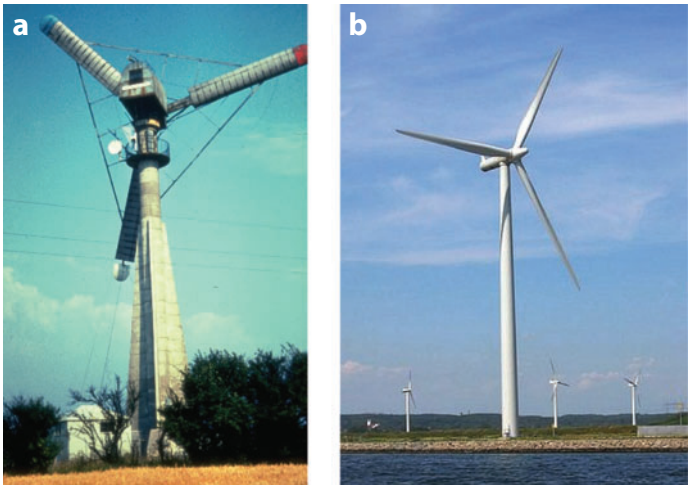

Figure 1

(*a*) The 200-kW Gedser turbine (1957). (*b*) A modern 2.5-MW wind turbine located in a cluster.

with models for wind conditions and structural dynamics. The integrated aeroelastic model for predicting performance and structural deflections is a prerequisite for the design, development, and optimization of wind turbines. Aerodynamic modeling also concerns the design of specific parts of wind turbines, such as rotor-blade geometry, and the performance predictions of wind farms.

The aerodynamics of wind turbines is in many ways different from the aerodynamics of fixed-wing aircraft or helicopters, for example. Whereas aerodynamic stall is always avoided for aircraft, it is an intrinsic part of the wind turbine's operational envelope. When boundary layer separation occurs, the centrifugal force tends to pump the airflow at the blade toward the tip, resulting in the aerodynamic lift being higher than what it would be on a nonrotating blade. Wind turbines are subjected to atmospheric turbulence, wind shear from the ground effect, wind directions that change both in time and in space, and effects from the wake of neighboring wind turbines. As a consequence, the forces vary in time and space, and a stochastic description of the wind field and a dynamical description of the blades and solid structures of the wind turbine are intrinsic parts of the aerodynamic analysis.

In recent years, most aerodynamic research has focused on establishing detailed experimental data and solving the incompressible Navier-Stokes equations for single rotors as well as for wind turbines located in complex terrain and for clusters of wind turbines. Although such computations are so heavy that they cannot be integrated directly in the design process, they may aid the designer of wind turbines in understanding the basic physics and in establishing engineering rules in combination with conventional design codes, such as the blade-element momentum (BEM) technique.

The following sections present some of the most important aerodynamic research topics within the field of wind energy. It is not possible to cover all aspects of rotor aerodynamics, so we focus on aerodynamic modeling, as it is used by industry in the design of new turbines, and on state-of-the-art methods for analyzing wind turbine rotors and wakes. Specifically, the basics of momentum theory, which still forms the backbone in rotor design for wind turbines, are introduced along with recent results from computational fluid dynamics (CFD) simulations of wind turbines and wind turbine wakes.

3. MOMENTUM THEORY AND BLADE-ELEMENT ANALYSIS

3.1. Basics of Momentum Theory

The basic tool for understanding wind turbine aerodynamics is the momentum theory in which the flow is assumed to be inviscid, incompressible, and axisymmetric. The momentum theory basically consists of control volume integrals for conservation of mass, axial and angular momentum balances, and energy conservation:

$$\oint_{CV} \rho \mathbf{V} \cdot d\mathbf{A} = 0, \tag{1}$$

$$\oint_{CV} u_x \rho \mathbf{V} \cdot d\mathbf{A} = T - \oint_{CV} p d\mathbf{A} \cdot \mathbf{e_x}, \tag{2}$$

$$\oint_{CV} r u_\theta \rho \mathbf{V} \cdot d\mathbf{A} = Q, \tag{3}$$

$$\oint_{CV} \left[p/\rho + \frac{1}{2} \|\mathbf{V}\|^2 \right] \rho \mathbf{V} \cdot d\mathbf{A} = P, \tag{4}$$

where $\mathbf{V} = (u_x, u_r, u_\theta)$ is the velocity vector in the axial, radial, and azimuthal direction, respectively; r is the radius; ρ is the density of air; $\mathbf{A}$ denotes the outward-pointing area vector of the control volume; p is the pressure; T is the axial force (thrust) acting on the rotor; Q is the torque; and P is the power extracted from the rotor.

The main dimensionless parameters to characterize the aerodynamic operation of a wind turbine are the following:

$$\text{Tip-speed ratio: } \lambda = \frac{\Omega R}{U_0}, \tag{5}$$

$$\text{Thrust coefficient: } C_T = \frac{T}{\frac{1}{2}\rho A U_0^2}, \tag{6}$$

$$\text{Power coefficient: } C_P = \frac{P}{\frac{1}{2}\rho A U_0^3}, \tag{7}$$

where Ω is the angular velocity of the rotor, A is the rotor area, R is the radius of the rotor, and U_0 is the wind speed.

Based on the simple one-dimensional (1D) momentum theory developed by Rankine (1865), W. Froude (1878), and R.E. Froude (1889), Betz (1920) showed that the power that can be extracted from a wind turbine is given by

$$C_P = 4a(1-a)^2, \tag{8}$$

where $a = 1 - u/U_0$ is referred to as the axial interference factor, and u denotes the axial velocity in the rotor plane. Differentiating the power coefficient with respect to the axial interference factor, the maximum obtainable power is given as $C_{P\max} = 16/27 \simeq 0.593$ for $a = 1/3$. This result is usually referred to as the Betz limit or the Lanchester-Betz-Joukowsky limit, as recently proposed by van Kuik (2007), and states the upper maximum for power extraction, which is that no more than 59.3% of the kinetic energy contained in a stream tube having the same cross section as the disc area can be converted to useful work by the disc. However, it does not include the losses due to rotation of the wake, and therefore it represents a conservative upper maximum.

Applying the axial momentum equation on a differential element (i.e., an annulus comprised by two stream surfaces), we get

$$\Delta T = \rho u \Delta A (U_o - u_1) + \Delta X, \tag{9}$$

where u_1 is the axial velocity in the wake, ΔA is the area of the rotor disk on which the local thrust ΔT acts, and ΔX denotes the axial component of the force exerted by the pressure on the annular control volume,

$$\Delta X = \oint_{CV} p d\mathbf{A} \cdot \mathbf{e_x}. \tag{10}$$

This term is usually neglected in BEM theory, as shown below, but as discussed by Goorjian (1972), for example, the term is not zero. Maintaining the term and combining it with Equations 1–4, we get the following equation:

$$\frac{u}{\frac{1}{2}(U_o + u_1)} = \left[1 - \frac{\Delta X}{\Delta T}\right] \cdot \left[1 - \frac{(p_o - p_1) + \frac{1}{2}\rho(u_{\theta_1}^2 - u_\theta^2)}{(p^+ - p^-)}\right]^{-1}, \tag{11}$$

where p_0 is the ambient pressure, u_θ is the azimuthal velocity just behind the rotor, the subscript i refers to the wake, and $(p^+ - p^-)$ is the pressure jump over the rotor disc (Sørensen & Mikkelsen 2001). To quantify the influence of neglecting some of the terms in the equation, Sørensen & Mikkelsen (2001) carried out a validation study using the numerical actuator disc model of Sørensen & Kock (1995). From the computations, they found that the term in the last bracket is very small, on the order of 10^{-3}, and may be ignored, whereas the term $\Delta X/\Delta T$ attains values of approximately 5%. Combining Equations 4, 7, and 11, we get

$$C_P = 4(1-a)^2 \left(a - \frac{\Delta X}{\Delta T}\right) \Big/ \left(1 - \frac{\Delta X}{\Delta T}\right)^2, \tag{12}$$

from which it is seen that the attainable power extraction is reduced as compared to a model ignoring the lateral force component from the pressure. Indeed, differentiating Equation 12 with respect to a, we get

$$C_{P\max} = \frac{16}{27}\left(1 - \frac{\Delta X}{\Delta T}\right) \quad \text{for} \quad a = \frac{1}{3}\left(1 + 2\frac{\Delta X}{\Delta T}\right), \tag{13}$$

showing that the maximum power coefficient reduces with an amount corresponding to $\Delta X/\Delta T$.

3.2. Blade-Element Momentum Theory

The BEM method was developed by Glauert (1935) as a practical way to analyze and design rotor blades. The basic approximations of the model are the assumptions that $u_\theta^2 \simeq u_{\theta 1}^2$, $p_0 \simeq p_1$, and $u \simeq \frac{1}{2}(U_0 + u_1)$. In the BEM theory, the loading is computed by combining local blade-element considerations using tabulated 2D airfoil data with 1D momentum theory. Introducing the azimuthal interference factor, $a' = \frac{u_\theta}{2\Omega r}$, and the flow angle ϕ, defined as the angle between the rotor plane and the relative velocity, the following relations determine the flow properties:

$$a = \frac{1}{4\sin^2\phi/(\sigma C_n) + 1}, \tag{14}$$

$$a' = \frac{1}{4\sin\phi\cos\phi/(\sigma C_t) - 1}, \tag{15}$$

where $\sigma = N_b c/2\pi r$ is the solidity of the rotor, and C_n and C_t denote the 2D normal and tangential force coefficients, respectively.

The BEM method is a 1D approach, corresponding to a rotor with an infinite number of blades. To account for the difference in circulation between an N_b-bladed rotor and an actuator disc, Prandtl (Betz 1919) derived a tip-loss factor, which Glauert (1935) introduced in the BEM technique. Glauert's method introduces a correction factor, F, as follows:

$$F = \frac{2}{\pi}\cos^{-1}\left[\exp\left(-\frac{N_b(R-r)}{2r\sin\phi}\right)\right], \tag{16}$$

where N_b denotes the number of blades and $(R - r)$ is the distance from the tip to the considered radial cross section. The correction is introduced by dividing the force coefficients in Equations 14 and 15 by F. Different tip-loss correction models have been developed to calculate the load and power of wind turbines (de Vries 1979). Recently, some existing tip-loss correction models were analyzed by Shen et al. (2005a,b), who found an inconsistency in their basic form, which results in incorrect predictions of the aerodynamic behavior in the proximity of the tip. To remedy the inconsistency, they proposed a new tip-loss correction model and tested it in combination with both a standard BEM model (Shen et al. 2005a) and a Navier-Stokes-based actuator disc model (Shen et al. 2005b).

When the axial interference factor becomes greater than approximately 0.4, the rotor starts to run in the turbulent wake state, and axial momentum theory is no longer valid (e.g., see Sørensen et al. 1998, Stoddard 1977). In the turbulent wake state, the momentum equation is replaced by an empirical relationship between the thrust coefficient and the axial interference factor. Different relations can be used (e.g., Eggleston & Stoddard 1987, Spera 1994, or Wilson & Lissaman 1974).

Dynamic wake or dynamic inflow refers to unsteady flow phenomena that affect the loading on the rotor. In a real flow situation, the rotor is subject to unsteadiness from coherent wind gusts, yaw misalignment, and control actions, such as pitching and yawing. An initial change creates a change in the distribution of trailing vorticity, which then is advected downstream and therefore first can be felt in the induced velocities after some time. In its simple form, the BEM method is basically steady; hence yaw and unsteady effects have to be included as additional add-ons. In the European CEC Joule II project "Dynamic Inflow: Yawed Conditions and Partial Span Pitch" (see Schepers & Snel 1995), various dynamic inflow models were developed and tested.

To include a realistic wind input in the computations, it is important to simulate a time history of the wind field that mimics a correct spatial and temporal variation. Veers (1988) developed a method for simulating the time history of the wind as it is seen by a rotating blade. In a later method by Mann (1998), cross-correlation features are obeyed by using the linearized Navier-Stokes equations as a basis for the model.

3.3. Airfoil Data

As a prestep to the BEM computations, 2D airfoil data have to be established from wind-tunnel measurements or computations. For many years, wind turbine blades were designed using well-tested aviation airfoils, such as the NACA 44xx and the NACA 63-4xx airfoils. However, since the beginning of the 1990s, various tailor-made airfoils have been designed for wind turbine rotors (e.g., Björk 1990, Fuglsang & Bak 2004, Tangler & Somers 1995, Timmer & van Rooij 1992). The basis for most designs is an optimization procedure combined with a 2D aerodynamic design code, such as the viscous-inviscid interactive XFOIL code (Drela 1989). Typically, airfoils are designed using optimization criteria that depend on the spanwise position on the blade and the type of turbine (i.e., if it is stall-regulated or pitch-regulated). For all optimizations, however, the airfoil has to be insensitive to leading-edge roughness.

To construct a set of airfoil data to be used for a rotating blade, the airfoil data further need to be corrected for 3D and rotational effects. Simple correction formulas for rotational effects have been proposed by Snel et al. (1993), Du & Selig (1998), Chaviaropoulos & Hansen (2000), and Bak et al. (2006) for incidences up to stall. As a simple engineering method, the following expression can be used to correct the lift data:

$$C_{l,3D} = C_{l,2D} + a(c/r)^b [C_{l,inv} - C_{l,2D}], \tag{17}$$

where a and b are constants, with a taking values from 2 to 3 and b from 1 to 2. A similar expression can be used for the drag coefficient. For higher incidences (>45°), 2D lift and drag coefficients of a flat plate can be used. These data, however, are too big because of aspect-ratio effects, and here the correction formulas of Viterna & Corrigan (1981) are usually applied (see also Spera 1994). Hoerner (1965) states that the normal coefficient is approximately constant for angles of attack between 45° and 90° and that the suction peak at the leading edge always causes a small driving force. Thus, as a guideline for the construction of airfoil data at high incidences, one can exploit the following features:

$$C_n = C_l \cos\phi + C_d \sin\phi = C_d(\alpha = 90°), \tag{18}$$

$$C_t = C_l \sin\phi - C_d \cos\phi > 0, \tag{19}$$

where a typical value for $C_d(\alpha = 90°)$ is 1.2. For angles of attack between stall and 45°, the airfoil data may be determined using linear interpolation between the two sets of corrected data.

An alternative to correcting 2D airfoil data is to obtain the 3D data directly from rotor experiments or from computations of rotor blades. One approach is to assume a similarity solution for the velocity profiles in the spanwise direction and then derive a set of quasi-3D flow equations. This idea has been exploited by Snel & van Holten (1995), Shen & Sørensen (1999), and Chaviaropoulos & Hansen (2000) using different approximations to the 3D Navier-Stokes equations that allow the Coriolis and centrifugal terms to be present in a 2D airfoil code. Hansen et al. (1997) and Johansen & Sørensen (2004) derived the local airfoil characteristics from full 3D CFD rotor computations using the azimuthally averaged velocity and the forces on the blade to extract lift and drag coefficients.

Apart from using CFD techniques, the angle of attack and airfoil data can be estimated from rotor experiments by combining pressure measurements with flow fields measured using hot-wire anemometry, particle image velocimetry, or laser Doppler anemometer techniques, for example. If only pressure measurements are available, however, then one must determine the induced velocity from a wake model. Local tangential and axial forces can be obtained directly from pressure measurements ignoring viscous effects, whereas obtaining lift and drag coefficients requires knowledge about the local angle of attack. Tangler (2004) and Sant et al. (2006) employed prescribed wake models to derive angle-of-attack distributions from the measured C_n and C_t values on the NREL Phase VI rotor. A free wake vortex model was further developed (Sant et al. 2009) to determine the angle of attack for a rotor operating in yaw. A general method for determining the angle of attack was recently developed by Shen et al. (2009a). The idea behind the technique is to employ the Biot-Savart integral to determine the influence of the bound vorticity on the local velocity field. The angle of attack is then calculated at some monitor point close to the blade section by subtracting the induction of the bound circulation from the velocity field.

As the angle of attack is constantly changing because of fluctuations in the wind and control actions, one must include a dynamic stall model to compensate for the time delay associated with the dynamics of the boundary layer and wake of the airfoil. This effect can be simulated by a simple first-order dynamic model, as proposed by Øye (1991a), or by a considerably more advanced model, taking into account attached flow and leading-edge separation as well, as in the

model of Larsen et al. (2007), and compressibility effects, as in the model of Leishman & Beddoes (1989).

4. OPTIMUM PERFORMANCE OF WIND TURBINE ROTORS

One way of capturing more energy from the wind is to improve the aerodynamic efficiency of the energy conversion by using optimization techniques in the initial design. Although wind turbine aerodynamics has been studied for nearly a century, optimum rotor design continues to be an important issue. From the Betz limit, it is known that no more than 59.3% of the available energy can be captured from a wind turbine. However, this is based on an idealized rotor with infinitely many blades and an analysis in which the rotational losses in the wake are ignored. In practice the aerodynamic performance will be reduced because of wake and tip losses, boundary layer drag, and nonideal inflow conditions. The following presents a brief overview of different optimum rotor models.

4.1. Infinite-Bladed Actuator Disc Models

A first extension of the axial momentum theory is to include rotational velocities and angular momentum in the analysis, assuming an actuator with infinitely many blades.

4.1.1. The optimum rotor of Glauert. Utilizing general momentum theory, Glauert (1935) developed a simple model for the optimum rotor that included rotational velocities. This approach treats the rotor as a rotating axisymmetric actuator disk, corresponding to a rotor with an infinite number of blades. The main approximation in Glauert's analysis was to ignore the influence of the azimuthal velocity and the term ΔX in the axial momentum given in Equation 9. Glauert (1935) derived the following equation for the power coefficient:

$$C_P = 8\lambda^2 \int_0^1 a'(1-a)x^3 dx, \tag{20}$$

where $x = r/R$. By assuming that the different stream tube elements behave independently, it is possible to optimize the integrand for each x separately (see Glauert 1935, Wilson & Lissaman 1974). This results in the following relation for an optimum rotor:

$$a' = \frac{1-3a}{4a-1}. \tag{21}$$

The analysis shows that the optimum axial interference factor is no longer a constant but will depend on the rotation of the wake and that the operating range for an optimum rotor is $1/4 \leq a \leq 1/3$. The maximal power coefficient as a function of tip-speed ratio is determined by integrating Equation 20 and is shown in **Table 1**. The optimal power coefficient approaches 0.593 at large tip-speed ratios only.

4.1.2. The constant circulation model of Joukowsky. About a century ago, Joukowsky (1912) developed a simple aerodynamic model based on general momentum theory and the concept of a rotor disc with constant circulation. This model has since been the subject of much controversy because it causes a power coefficient that, independent of tip-speed ratio, always is greater than

Table 1 Power coefficient as function of tip-speed ratio for optimum actuator disc

λ	0.5	1.0	1.5	2.0	2.5	5.0	7.5	10.0
$C_{P\max}$	0.288	0.416	0.480	0.512	0.532	0.570	0.582	0.593

16/27 and that, for small tip-speed ratios, tends to infinity. The model essentially consists of a constant axial flow superposed on a free vortex of strength $\Gamma = 2\pi r u_\theta$. Glauert (1935) states that the condition of constant circulation cannot be fully realized in practice as it implies that, near the roots of the blades, the angular velocity imparted to the air is greater than the angular velocity of the propeller itself. Other investigators, such as de Vries (1979) and Wilson & Lissaman (1974), shared Glauert's viewpoint that the solution is unphysical as it results in infinite values of power and circulation when the tip-speed ratio tends to zero. In a recent work, Sharpe (2004) argues that the theory in principle establishes that there is no loss of efficiency associated with the rotating wake and that it is possible, at least in theory, to exceed the Betz limit. Comments on Sharpe's analysis were published by Lam (2006) and Xiros & Xiros (2007). Furthermore, Wood (2007) published an approximate analysis of the same problem including the core radius of the hub vortex as well. From their analyses, they all conclude that the maximum power coefficient always is greater than the Betz limit of 16/27 and that it increases toward infinity with decreasing tip-speed ratio. However, in recent numerical studies on optimum rotors by Madsen et al. (2007) and Johansen et al. (2009), the optimum power coefficient did not exceed the Betz limit. Thus, there seems not be full agreement on the validity of the model. Recently, Sørensen & van Kuik (2010) came up with a possible explanation of the problem. In all analyses so far, the lateral pressure term ΔX is ignored in the momentum equation. If this term is included, the area expansion is reduced, which seems to solve the problem. From Equation 9, the wake expansion can be determined as follows:

$$\left(\frac{R_1}{R}\right)^2 = \frac{u}{u_1} = \frac{2\lambda q}{2\lambda q\left(1 - \frac{\Delta X}{\Delta T}\left(1 + \frac{q}{2\lambda}\right)\right) - b^2}, \tag{22}$$

where R_1/R is the ratio between the wake radius and the rotor radius, $q = \Gamma/(2\pi R U_0)$ is the dimensionless circulation, and $b = 1 - u_1/U_0$ is the axial wake interference factor (Sørensen & van Kuik 2010). Applying Equations 1 and 4, we can determine the circulation as

$$q = -\lambda\left(\frac{R}{R_1}\right)^2 + \left(\frac{R}{R_1}\right)\sqrt{\left(\frac{R}{R_1}\right)^2\lambda^2 + b(2-b)}, \tag{23}$$

and from the angular momentum equation, we get

$$C_P = 2\lambda q\left(\frac{R_1}{R}\right)^2(1-b). \tag{24}$$

Solving Equations 22–24, we can obtain the power coefficient for any combination of tip-speed ratio, axial wake interference factor, and lateral pressure component. **Figure 2** depicts the maximum power coefficient as a function of tip-speed ratio for different $\Delta X/\Delta T$ values and compares them to the optimum curve of Glauert. The lateral pressure largely influences the behavior of the maximum power coefficient. Ignoring the lateral pressure component (i.e., setting $\Delta X/\Delta T = 0$), it is clearly seen that $C_P \to \infty$ for $\lambda \to 0$. For $\Delta X/\Delta T \leq 0.1$, the C_P curve still has a hump, but for larger $\Delta X/\Delta T$ values, it goes monotonously toward the Betz limit. Thus, a likely explanation for the large increase in C_P at small tip-speed ratios is the lack of the lateral pressure on the control volume.

As shown in the previous analysis, the use of the axial momentum equation involves an additional unknown, the lateral pressure, which may greatly influence the solution. This problem may be avoided by neglecting the area expansion in Equations 23 and 24. In this case the inclusion of the momentum equation is not needed, and the power coefficient is simply written as

$$C_P = 4a(1-a)^2\frac{\lambda}{\lambda + \frac{1}{2}q}, \tag{25}$$

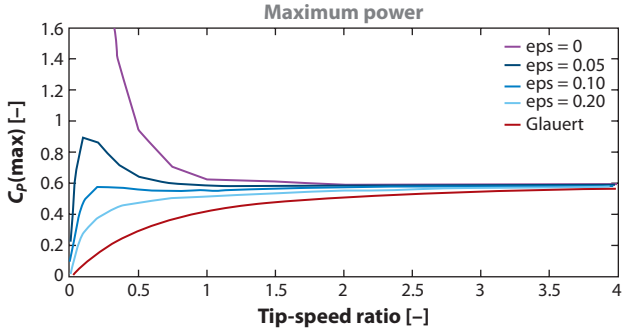

Figure 2

Maximum power coefficient of a Joukowsky rotor as a function of tip-speed ratio and lateral force component. The different $\Delta X/\Delta T$ values are denoted by eps. Figure adapted from Sørensen & van Kuik (2010).

with q determined from Equation 18 setting $R \simeq R_1$ (see Madsen et al. 2007, Sørensen & van Kuik 2010). It interesting that the term involving the tip-speed ratio acts as a simple modification of the rotation of the wake on the expression derived from 1D momentum theory (see Equation 8).

4.2. Finite-Bladed Rotor Models

In the history of rotor aerodynamics, two schools have dominated the conceptual interpretation of the optimum rotor. In Russia, Joukowsky (1912) defined the optimum rotor as one having constant circulation along the blades, such that the vortex system for an N_b-bladed rotor consists of N_b helical tip vortices of strength Γ and an axial hub vortex of strength $-N_b\Gamma$. A simplified model of this vortex system can be obtained by representing it as a rotating horseshoe vortex (see **Figure 3*a***). The other school, which essentially was formed by Prandtl and Betz (1919), showed that optimum efficiency is obtained when the distribution of circulation along the blades generates a rigidly helicoidal wake that moves in the direction of its axis with a constant velocity (**Figure 3*b***).

Based on Betz's (1919) conceptual idea, Goldstein (1929) developed a theory for lightly loaded propellers using infinite series of Bessel functions. Goldstein's theory was later generalized by Theodorsen (1948) to cover cases of heavily loaded propellers. Theodorsen (1948), however,

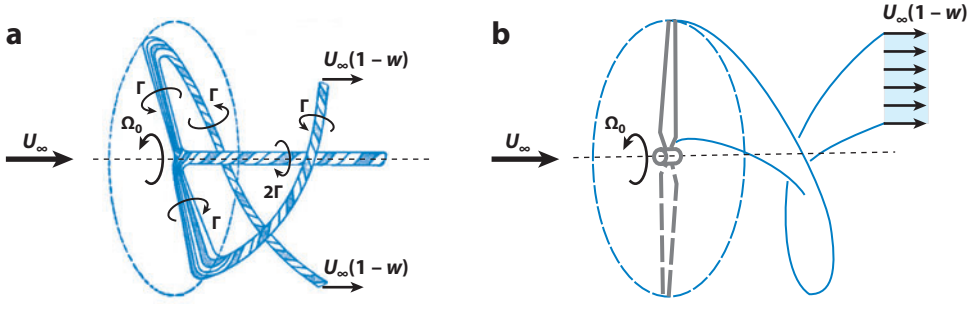

Figure 3

Sketch of the vortex system corresponding to lifting line theory of the ideal propeller of (*a*) Joukowsky and (*b*) Betz. Figure adapted from Okulov & Sørensen (2010).

employed a steady-control volume analysis for a wake that essentially is unsteady. Later contributions of the theory are due to Tibery & Wrench (1964), Sanderson & Archer (1983), Ribner & Foster (1990), Schouten (1992, 1999), Wald (2006), Verhoeff (2005), and Okulov & Sørensen (2008). An extension of Betz's (1919) criterion was recently proposed by Chattot (2003), who combined a general condition for minimum energy loss with a vortex lattice method.

Using the analytical solution to the induction of helical vortex filaments developed by Okulov (2004), Okulov & Sørensen (2008) analyzed in detail Goldstein's (1929) original formulation and found that, by a simple modification, the model can be extended to handle heavily loaded rotors in a way that is in full accordance with the general momentum theory. Assuming that the induction in the rotor plane equals half the induction in the Trefftz plane in the far wake, the power coefficient is written as

$$C_P \equiv \frac{P}{\frac{1}{2}\rho\pi R^2 U_0^3} = 2\bar{w}\left(1-\frac{1}{2}\bar{w}\right)\left(I_1-\frac{1}{2}\bar{w}I_3\right), \tag{26}$$

where $\bar{w} = w/U_0$ is the dimensionless translational velocity of the vortex sheet, and

$$I_1 = 2\int_0^1 G(x,l)\,x\,dx \quad \text{and} \quad I_3 = 2\int_0^1 G(x,l)\frac{x^3\,dx}{x^2+l^2}, \tag{27}$$

where $x = r/R$, $l = h/2\pi R$ is the dimensionless pitch of the vortex sheet, and $G(x,l) = N_b\Gamma(x,l)/hw$ denotes the Goldstein circulation function.

Figure 4*a* depicts the optimum power coefficient as a function of tip-speed ratio for different numbers of blades, whereas **Figure 4*b*** depicts the corresponding thrust coefficient. It is evident that the optimum power coefficient has a strong dependency on the number of blades. The comparison further shows that the results from the present theory for $N_b = \infty$ are in excellent agreement with the values computed from general momentum theory.

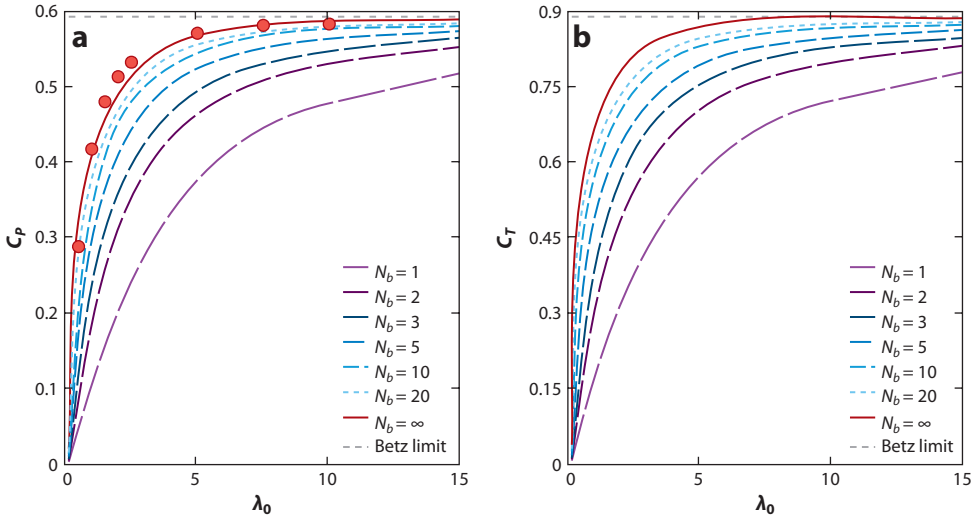

Figure 4

(*a*) Power coefficient, C_P, and (*b*) thrust coefficient, C_T, as a function of tip-speed ratio for different numbers of blades of an optimum rotor. Points represent the general momentum theory (**Table 1**), and dashed and solid lines represent the present theory. Figure adapted from Okulov & Sørensen (2008).

In Joukowsky's vortex theory, each rotor blade is replaced by a lifting line about which the circulation associated with the bound vorticity is constant. This results in a free vortex system consisting of helical vortices trailing from the tips of the blades and a rectilinear hub vortex. Exploiting the analytical solution to the induction of helical vortex filaments developed by Okulov (2004) and Fukumoto & Okulov (2005), and assuming that the convective velocity of the vortex system equals half of the averaged induced velocity in the wake, Okulov & Sørensen (2010) derived the following expression for the power coefficient:

$$C_P = 2a\left(1 - \frac{1}{2}a\,J_1\right)\left(1 - \frac{1}{2}a\,J_3\right), \tag{28}$$

where $J_1 = 1 + \sigma$ and $J_3 = 2\int_0^1 \tilde{u}(x,0)x\,dx$, with $\tilde{u} = u/(aU_0)$ denoting the nondimensional axial velocity in the Trefftz plane. Comparing the performance of the Joukowsky model with the Betz model, we find that the optimum power coefficient of the Joukowsky rotor for all numbers of blades is larger than that for the Betz rotor. The difference, however, vanishes for $\lambda \to \infty$ or for $N_b \to \infty$, for which both models tend toward the Betz limit.

4.3. A Simple Model Including Drag

To come up with a quick estimate of the maximum power coefficient that can be achieved with a given potential rotor configuration, Wilson et al. (1976) derived the following simple formula:

$$C_{P,\max} = \frac{16}{27}\lambda\left[\frac{N_b^{2/3}}{1.48 + (N_b^{2/3} - 0.04)\lambda + 0.0025\lambda^2} - \left(\frac{C_d}{C_l}\right)\frac{1.92N_b\lambda}{1 + 2\lambda N_b}\right]. \tag{29}$$

The model is based on a fit to Glauert's (1935) optimum actuator disk model and includes airfoil drag and the influence of a finite number of blades through the tip correction. Their fit to the data is accurate to within 0.5% for tip-speed ratios from 4 to 20, drag-to-lift ratios C_d/C_l from 0 to 0.04, and from one to three blades, according to Manwell et al. (2002).

4.4. Optimization Toward Minimizing Cost of Energy

More general optimizations of wind turbines include both aerodynamics and structural mechanics and aim to minimize the cost price of the produced energy. Thus, accurate and efficient models for predicting wind turbine performance are essential for obtaining reliable optimum designs of wind turbine rotors. The first multidisciplinary optimization method for designing horizontal-axis wind turbines is due to Fuglsang & Madsen (1999). Their method's objective was to minimize the cost of energy employing multiple constraints. Generally, multi-objective optimization methods are employed in which the blades are optimized by varying blade structural parameters such as stiffness, stability, and material weight. Site-specific features of wind farms (such as normal flat terrain and offshore and complex terrain) can also be incorporated in the design process of the wind turbine rotors, as shown by Fuglsang & Thomsen (2001). In a recent work, Xudong et al. (2009) demonstrated that it was possible to reduce the cost of energy by a few percent through the use of optimization techniques. However, it is important to emphasize that the optimization is no better than the aerodynamic model used, which up to now has been based on the BEM technique.

5. ADVANCED ROTOR AERODYNAMICS

On the basis of various empirical extensions, the BEM method has developed into a rather general design and analysis tool that is capable of coping with all kinds of flow situations. Owing to its

simplicity and generality, it is today the only design methodology in use by industry. There is, however, a need to develop more sophisticated models to provide airfoil data and to understand more fundamentally the underlying physics of rotary flows. Furthermore, available computer resources are steadily increasing, which makes it possible to incorporate more comprehensive aerodynamics prediction tools in the design process. As a consequence, various simulation models have been developed and employed to study the aerodynamics of wind turbine rotors and dynamics of wakes. The models range from simple lifting line wake models to Navier-Stokes CFD models, using either generalized actuator disc hypotheses or full rotor simulations. The following discussion presents the state of the art of advanced numerical simulation tools for wind turbine rotors and wakes.

5.1. Computations of Wind Turbine Rotors

Since the 1970s a strong research activity within the aeronautical field has resulted in the development of a series of CFD tools based on the solution of the Euler or Navier-Stokes equations. The models range from simple panel models and hybrid viscous-inviscid interactive codes to full-blown Navier-Stokes simulation tools.

In panel or vortex methods, the flow field is determined from the induction law of Biot-Savart, in which vortex filaments in the wake are advected by superposition of the undisturbed flow and the induced velocity field. The trailing wake is generated by spanwise variations of the bound vorticity along the blade. The shed wake is generated by the temporal variations as the blade rotates. Pure panel methods are of limited use for computing wind turbine rotors as the flow is dominated by viscous effects. However, coupled to a viscous-inviscid interactive procedure, they constitute an inexpensive alternative to heavy Navier-Stokes simulations. In the field of wind energy, hybrid viscous-inviscid methods have been applied by Sørensen (1986), Xu & Sankar (2000), and Voutsinas (2006).

Today, most development of advanced aerodynamic methods in wind energy concerns Navier-Stokes methods. Some of the experience gained from the aeronautical research institutions has been exploited directly in the development of CFD algorithms for wind turbines. Notable is the development of numerical schemes for the solution of the flow equations, efficient solution algorithms, grid-generation techniques, and models for boundary layer turbulence and laminar/turbulent transition.

Two main paths are typically followed when conducting CFD computations. Either the equations are time filtered, solving the so-called Reynolds-averaged Navier-Stokes equations (RANS), or they are space filtered, performing large-eddy simulations. In both cases, a part of the flow is modeled through a turbulence model. The advantage of RANS is that a fully resolved computation can be carried out with a few million mesh points, which makes it possible to reach a full 3D solution, even on a portable computer.

The first full Navier-Stokes simulation for a complete rotor blade was carried out by N.N. Sørensen & Hansen (1998) using the $k-\omega$ SST model of Menter (1993). These simulations were later followed by Duque et al. (1999, 2003) and N.N. Sørensen et al. (2002) in connection with the American NREL experiment at NASA Ames and the accompanying NREL/NWTC Aerodynamics Blind Comparison test (Schreck 2002). The NREL experiments have achieved significant new insight into wind turbine aerodynamics and revealed serious shortcomings in present-day wind turbine aerodynamics prediction tools. In particular it was found that performance computations using the BEM technique were extremely sensitive to the input blade section aerodynamic data. The Navier-Stokes computations generally exhibited good agreement with the measurements up to wind speeds of approximately 10 m s^{-1}. At this wind speed, flow separation sets in, and for higher

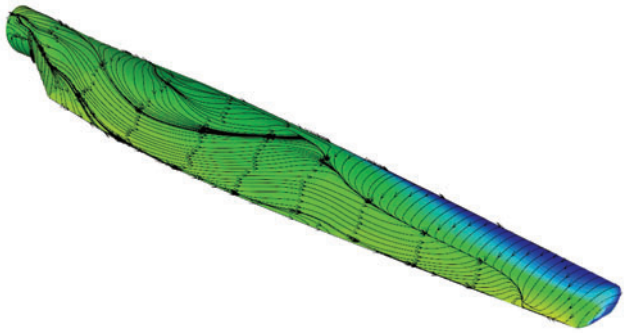

Figure 5

Computed limiting streamlines and pressure contours on the NREL 5MW rotor.

wind speeds, the boundary layer characteristics are dominated by stall and the computations underpredict the power yield. Johansen et al. (2002) applied a hybrid large-eddy simulation/RANS technique on the NREL phase VI rotor under parked conditions. Good agreement with measurements was obtained at low angles of attack when the flow largely is attached. However, at high angles of attack, the computations did not improve as compared to RANS computations. In the conclusion it was suggested the inclusion of a laminar/turbulent transition model most likely will improve the quality of the results. To this end, a recent study by Sørensen (2009), using the correlation-based transition model of Menter et al. (2004), showed that a proper transition model indeed improves the results, but the results at high wind speeds still underpredict the power.

A number of full 3D Navier-Stokes computations have been carried out to study various aspects of rotor aerodynamics. Johansen & Sørensen (2004) derived airfoil characteristics from CFD computations, Madsen et al. (2003) and Tongchitpakdec et al. (2005) analyzed yaw, Hansen & Johansen (2004) carried out computations to study tip flows and validate tip-loss models for use in BEM theory, Chao & van Dam (2007) carried out computations to analyze a blunt-trailing-edge modification to the NREL Phase VI rotor, and Zahle et al. (2009) employed an overset grid method to analyze the interaction between the rotor blade and the tower. Commercial CFD codes have been employed by Carcangiu et al. (2007), Wussow et al. (2007), and Laursen et al. (2007) to demonstrate the potential of CFD use in the commercial wind industry. **Figure 5** shows limiting streamlines and pressure contours from a computation of the NREL 5MW rotor. The figure clearly illustrates the complicated streamline pattern associated with the separation of the boundary layer.

5.2. Simulation and Modeling of Wakes

Today most wind turbines are clustered in small groups or in wind farms to reduce space as well as installation and maintenance expenses. The interference between the wakes of the turbines, however, reduces the total power production as compared with an equal number of stand-alone turbines. Furthermore, the turbulence intensity between the turbines increases because of mixing from surrounding wakes, resulting in increased dynamic loadings. The turbulence in wind turbine wakes is mainly generated from the rotor loading and the dynamics of the vortices originating from the rotor blades. To analyze the genesis of the wake, it is thus necessary to include descriptions of the aerodynamics of both the rotor and the wake. Although many wake studies have been performed over the past two decades, many basic questions still need to be clarified to elucidate the dynamic behavior of individual as well as multiple interactive wakes behind wind turbines.

In a recent survey, Vermeer et al. (2003) discussed both near-wake and far-wake aerodynamics, whereas Crespo et al. (1999) presented a survey focusing solely on far-wake modeling.

Wind-tunnel investigations have been carried out by Ronsten (1992), Ebert & Wood (1997), Whale et al. (2000), Vermeer (2001), Medici & Alfredsson (2006), Massouh & Dobrev (2007), and Hans et al. (2008), among others. Valuable information on various aspects of wind turbine aerodynamics was obtained in the American NREL experiment at NASA Ames (Fingersh et al. 1995). Recently, the European-funded MEXICO wind-tunnel experiment concluded with detailed particle image velocimetry measurements in the wake of a 4.5-m diameter rotor (Snel et al. 2007). The project's main objective was to create a database of detailed aerodynamic measurements to be used for model validation and improvement of computing codes. Full-scale field tests have been reported by, e.g., Højstrup (1990), Øye (1991b), and Cleijne (1993) and in the IEA Annex XVIII database (Schepers et al. 2002). Recent progress in the lidar technique has opened new doors for detailed full-scale measurements of full flow fields (Bingol et al. 2010).

Axisymmetric far-wake models have been developed to describe the wake velocity after the initial expansion by Ainslie (1985, 1988). Ainslie's original formulation specified the inflow condition as a Gaussian velocity distribution. To include the velocity profile of the actual rotor, Larsen et al. (2008a) used the result from a BEM computation as a starting condition. Detailed numerical studies of far wakes have been carried out by Crespo & Hernández (1996) using methods based on the UPMWAKE model in which the wind turbine is immersed in an atmospheric boundary layer. This model uses a finite-difference approach and a parabolic approximation to solve the 3D RANS equations combined with a $k - \varepsilon$ turbulence model. An extension of the UPMWAKE model to cope with more wind turbines is the WAKEFARM model by ECN (Schepers & van der Pihl 2007), which divides the wake into a near and a far wake in which the turbulent processes in the far wake are modeled with a $k-\varepsilon$ turbulence model. As the parabolization of the Navier-Stokes equations only can be justified in the far wake, the near wake is described with various empirical approximations. Another extension, still within the assumption of parabolized equations, is to replace the $k - \varepsilon$ equations by an explicit algebraic turbulence model (Gómez-Elvira et al. 2005). This extension improved the previous isotropic models and gave a more accurate representation of the large-scale flow, even if the flow associated with these scales was not fully turbulent.

To study the details of the near wake, it is necessary to solve the fully elliptic equations and include the rotor in the computations. This demands a large number of mesh points, as both the details of the rotor boundary layer and the vortices in the wake need to be captured. Thus, in practice it is still beyond present computer capability to perform combined rotor/wake computations within an acceptable accuracy. As an alternative, one may replace the rotor by an actuator disc or an actuator line. In a numerical actuator disc/line model, the flow field is determined by solving the Navier-Stokes (or Euler) equations by a finite-difference/volume scheme and replacing the rotor by surface forces that act upon the incoming flow. The forces are implemented either at a rate corresponding to the mechanical work that the rotor extracts from the flow or by using local instantaneous values of tabulated airfoil data. For airfoils subjected to temporal variations of the angle of attack, the dynamic response of the aerodynamic forces changes the static airfoil data, and dynamic stall models have to be included. The first computations of wind turbine wakes employing numerical actuator disc models in combination with a blade-element approach were carried out by Sørensen & Myken (1992). Later studies using the actuator disc technique are due to Sørensen & Kock (1995), Madsen (1996), Masson et al. (2001), and Ammara et al. (2002). These studies were later followed by different research groups who employed the technique to study various flow cases, including coned and yawed rotors (Mikkelsen et al. 2001), rotors operating in enclosures (Hansen et al. 2000), wind turbines in atmospheric environments (Jimenez et al. 2007), wake meandering (Larsen et al. 2008b), and wind farm simulations (Calaf et al. 2010, Ivanell et al.

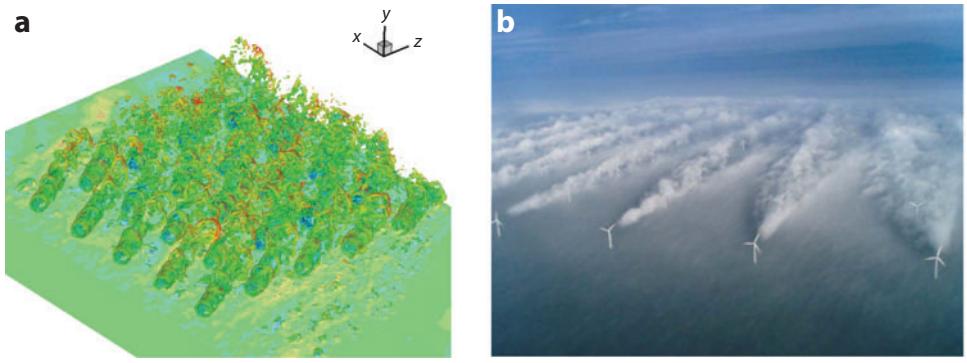

Figure 6

(*a*) Actuator disc computation of a wind farm consisting of 5 × 5 wind turbines. (*b*) Photograph showing the flow field around the Horns Rev wind farm.

2008). **Figure 6** shows a qualitative comparison between the flow field around the Horns Rev wind farm, as observed from a helicopter in the early morning, and a computation of a wind farm consisting of 5 × 5 wind turbines.

The main limitation of the actuator disc approach is that the forces are distributed evenly; hence the influence of the blades is taken as an integrated quantity in the azimuthal direction. To overcome this limitation, researchers developed extended 3D actuator line or surface models (Leclerc & Masson 2004, Shen et al. 2009b, Sibuet Watters & Masson 2007, Sørensen & Shen 2002). The concept enables one to study in detail the dynamics of the wake and the tip vortices and their influence on the induced velocities in the rotor plane. Wake studies using the actuator line technique have been reported by Mikkelsen et al. (2007), Ivanell et al. (2009), and Troldborg et al. (2010). Reviews of the basic modeling of actuator disc and actuator line models can be found in the Ph.D. dissertations of Mikkelsen (2003), Ivanell (2009), and Troldborg (2008).

6. FUTURE ISSUES

The aerodynamic research of wind turbines has contributed significantly to the success of modern wind energy. For most unsolved problems, engineering rules have been developed and verified. All these rules have limited applicability, and, in light of the rapid development of wind energy, the need to replace them with physical understanding and modeling based on computer simulations of the Navier-Stokes equations is increasing. Future research efforts are directed toward strong aeroelastic coupling between the flow field and the wind turbine. This demands the development of algorithms that combine structural dynamics and aerodynamic loading. Applications range from the analysis of specific parts of rotor blades (such as tip shapes, control mechanisms, and vortex generators) to detailed analyses of flow structures and stresses. Another important issue concerns the description of wake structures subject to atmospheric turbulence and the optimization of wind turbines clustered in parks. Here the limitations are dictated by limited computer power, and for many years it will be necessary to introduce various approximations, such as synthetic turbulence and body forces, to represent the actual behavior of the wind field and the rotor. Some of the classical problems still remain, such as laminar-turbulent transition and boundary layer turbulence. These problems, however, are common for the fluid mechanics society in general.

SUMMARY POINTS

1. The classical method for determining wind turbine aerodynamics—the BEM technique—is today employed with various add-ons for coping with complex 3D and unsteady effects. This makes it possible to cope with all realistic operational conditions of importance for the design of the rotor.
2. Airfoil data are derived from experiments and CFD computations using new techniques to determine the angle of attack.
3. An explanation for the anomalous behavior of Joukowsky's infinite-bladed rotor and new theories for optimum performance of finite-bladed rotors have been developed. These give some simple guidelines for how to design optimum rotors.
4. Most development of advanced aerodynamic methods in wind energy concerns CFD methods. However, as demonstrated by the NREL blind-test experiment, it is still not possible to achieve realistic results at high wind speeds at which most of the rotor boundary layer is separated.
5. Simulations of wakes and turbulence in wind farms are carried out using various approximations to the actual flow features. One method is to combine CFD techniques with an actuator line or actuator disc model in which the rotor blades are replaced by body forces and the incoming wind is simulated using synthetic turbulence.

DISCLOSURE STATEMENT

The author is not aware of any affiliations, memberships, funding, or financial holdings that might be perceived as affecting the objectivity of this review.

ACKNOWLEDGMENTS

The author wishes to acknowledge the efforts of coauthors and collaborators. In particular he wishes to thank Wen Zhong Shen, Martin O.L. Hansen, Robert Mikkelsen, Valery Okulov, Kurt S. Hansen, Stig Øye, Stefan Ivanell, and the group for Aeroelastic Design at Risø-DTU for their partnership over the years.

LITERAURE CITED

Ainslie JF. 1985. Development of an eddy viscosity model for wind turbine wakes. In *Proc. 7th BWEA Wind Energy Conference, Oxford*, pp. 61–66. London: Mech. Eng. Publ.

Ainslie JF. 1988. Calculating the field in the wake of wind turbines. *J. Wind Eng. Ind. Aerodyn.* 27:213–24

Ammara I, Leclerc C, Masson C. 2002. A viscous three-dimensional method for the aerodynamic analysis of wind farms. *J. Sol. Energy Eng.* 124:345–56

Bak C, Johansen J, Andersen PB. 2006. Three-dimensional corrections of airfoil characteristics based on pressure distributions. In *Proc. Eur. Wind Energy Conf. Exhib. (EWEC), Athens, Greece*, Pap. BL3.356. Brussels: Eur.Wind Energy Assoc.

Betz A. 1919. *Schraubenpropeller mit geringstem Energieverlust*. Diss. Gottingen Nachrichten, Gottingen

Betz A. 1920. Das Maximum der theoretisch möglichen Ausnützung des Windes durch Windmotoren. *Z. Gesamte Turbinenwesen* 26:307–9

Bingol F, Mann J, Larsen GC. 2010. Light detection and ranging measurements of wake dynamics, part I: one-dimensional scanning. *Wind Energy* 13:51–61

Björk A. 1990. Coordinates and calculations for the FFA-w1-xxx, FFA-w2-xxx and FFA-w3-xxx series of airfoils for horizontal axis wind turbines. *Tech. Rep. FFA TN 1990-15*, Stockholm

Brouckaert J-F, ed. 2007. *Wind Turbine Aerodynamics: A State-of-the-Art*. VKI Lect. Ser. 2007-05. Rhode Saint Genese, Belg.: von Kármán Inst. Fluid Dyn.

Calaf M, Meneveau C, Meyers J. 2010. Large eddy simulation study of fully developed wind-turbine array boundary layers. *Phys. Fluids* 22:015110

Carcangiu CE, Sørensen JN, Cambuli F, Mandas N. 2007. CFD-RANS analysis of the rotational effects on the boundary layer of wind turbine blades. *J. Phys. Conf. Ser.* 75:012031

Chao DD, van Dam CP. 2007. Computational aerodynamic analysis of a blunt trailing-edge airfoil modification to the NREL Phase VI rotor. *Wind Energy* 10:529–50

Chattot JJ. 2003. Optimization of wind turbines using helicoidal vortex model. *J. Sol. Energy Eng.* 125:418–24

Chaviaropoulos PK, Hansen MOL. 2000. Investigating three-dimensional and rotational effects on wind turbine blades by means of a quasi-3D Navier Stokes solver. *J. Fluids Eng.* 122:330–36

Cleijne JW. 1993. Results of the Sexbierum wind farm: single wake measurements. *Tech. Rep. TNO-Rep. 93-082*. Inst. Environ. Energy Technol., The Neth.

Crespo A, Hernández J. 1996. Turbulence characteristics in wind-turbine wakes. *J. Wind Eng. Ind. Aerodyn.* 61:71–85

Crespo A, Hernández J, Frandsen S. 1999. Survey of modelling methods for wind turbine wakes and wind farms. *Wind Energy* 2:1–24

de Vries O. 1979. Fluid dynamic aspects of wind energy conversion. *AGARDograph 243*, AGARD, Brussels

Drela M. 1989. XFOIL: an analysis and design system for low Reynolds number airfoils. In *Low Reynolds Number Aerodynamics*, ed. TJ Mueller. Lect. Notes Eng. 54. New York: Springer

Du Z, Selig MS. 1998. *A 3-D stall-delay model for horizontal axis wind turbine performance prediction*. Presented at AIAA Aerosp. Sci. Meet. Exhib., 36th, ASME Wind Energy Symp., Reno, AIAA Pap. No. 1998-21

Duque EPN, Burklund MD, Johnson W. 2003. *Navier-Stokes and comprehensive analysis performance predictions of the NREL phase VI experiment*. Presented at AIAA Aerosp. Sci. Meet. Exhib., 41st, Reno, AIAA Pap. No. 2003-355

Duque EPN, van Dam CP, Hughes S. 1999. *Navier-Stokes simulations of the NREL combined experiment phase II rotor*. Presented at AIAA Aerosp. Sci. Meet. Exhib., 37th, ASME Wind Energy Symp., Reno, AIAA Pap. No. 1999-37

Ebert PR, Wood DH. 1997. The near wake of a model horizontal-axis wind turbine: I. experimental arrangements and initial results. *Renew. Energy* 12:225–43

Eggleston DM, Stoddard FS. 1987. *Wind Turbine Engineering Design*. New York: Van Nostrand Rheinhold

Fingersh L, Simms D, Butterfield C, Jenks M. 1995. An overview of the Unsteady Aerodynamics Experiment Phase III data acquisition system and instrumentation. In *ASME Energy Environ. Expo*, *Houston*, pp. 277–280. New York: Am. Soc. Mech. Eng.

Froude W. 1878. *Trans. Inst. Naval Arch.* 19:47

Froude RE. 1889. *Trans. Inst. Naval Arch.* 30:390

Fuglsang P, Bak C. 2004. Development of the Risø wind turbine airfoils. *Wind Energy* 7:145–62

Fuglsang P, Madsen HA. 1999. Optimization method for wind turbine rotors. *J. Wind Eng. Ind. Aerodyn.* 80:191–206

Fuglsang P, Thomsen K. 2001. Site-specific design optimization of 1.5–2.0 MW wind turbines. *J. Sol. Energy Eng.* 123:296–303

Fukumoto Y, Okulov VL. 2005. The velocity field induced by a helical vortex tube. *Phys. Fluids* 17:107101

Glauert H. 1935. Airplane propellers. In *Aerodynamic Theory*, ed. WF Durand, vol. IV, Division L, pp. 191–269. New York: Springer

Goldstein S. 1929. On the vortex theory of screw propellers. *Proc. R. Soc. Lond. A* 123:440–65

Gomez-Elvira R, Crespo A, Migoya E, Manuel F, Hernandez J. 2005. Anisotropy of turbulence in wind turbine wakes. *J. Wind Eng. Ind. Aerodyn.* 93:797–814

Goorjian PM. 1972. An invalid equation in the general momentum theory of the actuator disc. *AIAA J.* 10:543–44

Hans W, Sant T, van Kuik G, van Bussel G. 2008. HAWT near-wake aerodynamics, part I: axial flow conditions. *Wind Energy* 11:245–64

Hansen MOL, Johansen J. 2004. Tip studies using CFD and comparison with tip loss models. *Wind Energy* 7:343–56
Hansen MOL, Sørensen NN, Flay RGJ. 2000. Effect of placing a diffuser around a wind turbine. *Wind Energy* 4:207–13
Hansen MOL, Sørensen NN, Sørensen JN, Michelsen JA. 1997. Extraction of lift, drag and angle of attack from computed 3-D viscous flow around a rotating blade. In *Proc. Eur. Wind Energy Conf. Exhib.* (*EWEC*), pp. 499–502. Brussels: Eur. Wind Energy Assoc.
Hoerner SF. 1965. *Fluid Dynamic Drag*. Brick Town, NJ: Hoerner Fluid Dyn.
Højstrup J. 1990. Wake measurements on the Nibe wind-turbines in Denmark. *Final Rep. CEC Contract EN3W.0039*, United Kingdom
Ivanell SA. 2009. *Numerical computations of wind turbine wakes*. PhD diss. KTH, Royal Inst. Technol., Stockholm
Ivanell S, Mikkelsen R, Sørensen JN, Henningson D. 2008. Three dimensional actuator disc modeling of wind farm wake interaction. In *Proc. 2008 Eur. Wind Energy Conf. Exhib*. Brussels: Eur. Wind Energy Assoc.
Ivanell S, Sørensen JN, Mikkelsen R, Henningson D. 2009. Analysis of numerically generated wake structures. *Wind Energy* 12:63–80
Jimenez A, Crespo A, Migoya E, Garcia J. 2007. Advances in large-eddy simulation of a wind turbine wake. *J. Phys. Conf. Ser.* 75:012041
Johansen J, Madsen HA, Gaunaa M, Bak C, Sørensen NN. 2009. Design of a wind turbine rotor for maximum aerodynamic efficiency. *Wind Energy* 12:261–74
Johansen J, Sørensen NN. 2004. Aerofoil characteristics from 3D CFD rotor computations. *Wind Energy* 7:283–94
Johansen J, Sørensen NN, Michelsen JA, Schreck S. 2002. Detached-eddy simulation of flow around the NREL phase VI blade. *Wind Energy* 5:185–97
Joukowsky NE. 1912. Vortex theory of a rowing screw. *Tr. Otd. Fiz. Nauk Obshchestva Lubitelei Estestvozn.* 16:1 (In Russian)
Lam GCK. 2006. Wind energy conversion efficiency limit. *Wind Eng.* 30:431
Larsen G, Madsen HA, Larsen TJ, Troldborg N. 2008a. Wake modeling and simulation. *Tech. Rep. Risø-R-1653*(*EN*), Risø Natl. Lab., Roskilde
Larsen G, Madsen HA, Thomsen K, Larsen TJ. 2008b. Wake meandering: a pragmatic approach. *Wind Energy* 11:377–95
Larsen JW, Nielsen SRK, Krenk S. 2007. Dynamic stall model for wind tubine airfoils. *J. Fluids Struct.* 23:959–82
Laursen J, Enevoldsen P, Hjort S. 2007. 3D CFD quantification of the performance of a multi-megawatt wind turbine. *J. Phys. Conf. Ser.* 75:012007
Leclerc C, Masson C. 2004. *Towards blade-tip vortex simulation with an actuator-lifting surface model*. Presented at AIAA Aerosp. Sci. Meet. Exhib., 42nd, Reno, AIAA Pap. No. 2004-667
Leishman JG, Beddoes TS. 1989. A semiempirical model for dynamic stall. *J. Am. Helicop. Soc.* 34(3):3–17
Madsen HA. 1996. A CFD analysis for the actuator disc flow compared with momentum theory results. In *Proc. 10th IEA Symp. Aerodyn. Wind Turbines*, pp. 109–24. Lyngby, Denmark: Tech. Univ. Denmark
Madsen HA, Mikkelsen R, Øye S, Bak C, Johansen J. 2007. A detailed investigation of the blade element momentum (BEM) model based on analytical and numerical results and proposal for modifications of the BEM model. *J. Phys. Conf. Ser.* 75:012016
Madsen HA, Sørensen NN, Schreck S. 2003. *Yaw aerodynamics analyzed with three codes in comparison with experiments*. Presented at AIAA Aerosp. Sci. Meet. Exhib., 41st, Reno, AIAA Pap. No. 2003-519
Mann J. 1998. Wind field simulation. *Probl. Eng. Mech.* 13:269–82
Manwell JF, McGowan JG, Rogers AL. 2002. *Wind Energy Explained*. New York: Wiley & Sons
Masson C, Smaili A, Leclerc C. 2001. Aerodynamic analysis of HAWTs operating in unsteady conditions. *Wind Energy* 4:1–22
Massouh F, Dobrev I. 2007. Exploration of the vortex wake behind of wind turbine rotor. *Phys. Conf. Ser.* 75:012036
Medici D, Alfredsson PH. 2006. Measurements on a wind turbine wake: 3D effects and bluff-body vortex shedding. *Wind Energy* 9:219–36

Menter FR. 1993. *Zonal two-equation k – ω models for aerodynamic flows*. Presented at AIAA Fluid Dyn., Plasmadyn., Lasers Conf., 23rd, Orlando, FL, AIAA Pap. No. 1993-2906

Menter FR, Langtry RB, Likki SR, Suzen YB, Huang PG, Völker S. 2004. A correlation-based transition model using local variables, part I: model formulation. In *Proc. ASME Turbo Expo 2004, Power Land, Sea, Air, Vienna, Austria*, GT2004-53452. New York: ASME

Mikkelsen R. 2003. Actuator disc methods applied to wind turbines. *Rep. MEK-FM PHD 2003-02*, Dep. Mech. Eng., DTU, Denmark

Mikkelsen R, Sørensen JN, Øye S, Troldborg N. 2007. Analysis of power enhancement for a row of wind turbines using the actuator line technique. *J. Phys. Conf. Ser.* 75:012044

Mikkelsen R, Sørensen JN, Shen WZ. 2001. Modeling and analysis of the flow field around a coned rotor. *Wind Energy* 4:121–35

Okulov VL. 2004. On the stability of multiple helical vortices. *J. Fluid Mech.* 521:319–42

Okulov VL, Sørensen JN. 2008. Refined Betz limit for rotors with a finite number of blades. *Wind Energy* 11:415–26

Okulov VL, Sørensen JN. 2010. Maximum efficiency of wind turbine rotors using Joukowsky and Betz approaches. *J. Fluid Mech.* In press

Øye S. 1991a. Dynamic stall, simulated as a time lag of separation. In *Proc. 4th IEA Sympos. Aerodyn. Wind Turbines, Harwell, UK*, ETSU-N-118. Harwell, UK: Harwell Lab.

Øye S. 1991b. Tjæreborg wind turbine, first dynamic inflow measurements. *Rep. AFM Notat VK-189*, Dep. Fluid Mech., DTU, Denmark

Rankine WJ. 1865. *Trans. Inst. Naval Archit.* 6:13

Ribner HS, Foster SP. 1990. Ideal efficiency of propellers: Theodorsen revisited. *AIAA J. Aircr.* 27:810–19

Ronsten G. 1992. Static pressure measurements on a rotating and a nonrotating 2·375 m wind turbine blade. Comparison with 2D calculations. *J. Wind Eng. Ind. Aerodyn.* 39:105–18

Sanderson RJ, Archer RD. 1983. Optimum propeller wind turbines. *J. Energy* 7:695–701

Sant T, van Kuik G, van Bussel GJW. 2006. Estimating the angle of attack from blade pressure measurements on the NREL phase VI rotor using a free-wake vortex model: axial conditions. *Wind Energy* 9:549–77

Sant T, van Kuik G, van Bussel GJW. 2009. Estimating the angle of attack from blade pressure measurements on the national renewable energy laboratory phase VI rotor using a free-wake vortex model: yawed conditions. *Wind Energy* 12:1–32

Schepers JG, Brand AJ, Bruining A, van Rooij R, Graham JMR, et al. 2002. Final report of IEA Annex VIII: enhanced field rotor aerodynamics database. *Rep. ECN-C-02-016*, The Neth.

Schepers JG, van der Pihl SP. 2007. Improved modelling of wake aerodynamics and assessment of new farm control strategies. *J. Phys. Conf. Ser.* 75:012039

Schouten G. 1992. Theodorsen's ideal propeller performance with ambient pressure in the slipstream. *J. Aircr.* 30:417–19

Schouten G. 1999. Theodorsen's propeller performance with rollup and swirl in the slipstream. *J. Aircr.* 36:892–95

Schreck S. 2002. The NREL full-scale wind tunnel experiment introduction to the special issue. *Wind Energy* 5:77–84

Sharpe DJ. 2004. A general momentum theory applied to an energy-extracting actuator disc. *Wind Energy* 7:177–88

Shen WZ, Hansen MOL, Sørensen JN. 2009a. Determination of the angle of attack on rotor blades. *Wind Energy* 12:91–98

Shen WZ, Mikkelsen R, Sørensen JN, Bak C. 2005a. Tip loss corrections for wind turbine computations. *Wind Energy* 8:457–75

Shen WZ, Sørensen JN. 1999. Quasi-3D Navier-Stokes model for a rotating airfoil. *J. Comput. Phys.* 150:518–48

Shen WZ, Sørensen JN, Mikkelsen R. 2005b. Tip loss corrections for actuator/Navier-Stokes computations. *J. Sol. Energy Eng.* 121:209–13

Shen WZ, Zhang JH, Sørensen JN. 2009b. The actuator surface model: a new Navier-Stokes based model for rotor computations. *J. Sol. Energy Eng.* 131:011002

Sibuet Watters C, Masson C. 2007. Recent advances in modeling of wind turbine wake vertical structure using a differential actuator disk theory. *J. Phys. Conf. Ser.* 75:012037

Snel H, Houwink R, van Bussel GJW, Bruining A. 1993. Sectional prediction of 3D effects for stalled flow on rotating blades and comparison with measurements. In *Proc. Eur. Comm. Wind Energy Conf.*, pp. 395–99. Lübeck-Travemünde, Germ.: H.S. Stephens & Assoc.

Snel H. Schepers JG. 1995. Joint investigation of dynamic inflow effects and implementation of an engineering method. *Rep. ECN-C-94-107*, Petten, The Neth.

Snel H, Schepers JG, Montgomerie B. 2007. The MEXICO (model experiments in controlled conditions): the database and first results of data process and interpretation. *J. Phys. Conf. Ser.* 75:012014

Snel H, van Holten T. 1995. Review of recent aerodynamic research on wind turbines with relevance to rotorcraft. *AGARD Rep. CP-552*, ch. 7, pp. 1–11

Sørensen JN. 1986. *Three-level viscous-inviscid interaction technique for the prediction of separated flow past rotating wind*. PhD diss. AFM 86-03, Dep. Fluid Mech., Tech. Univ. Denmark, Lyngby

Sørensen JN, Kock CW. 1995. A model for unsteady rotor aerodynamics. *J. Wind Eng. Ind. Aerodyn.* 58:259–75

Sørensen JN, Mikkelsen R. 2001. On the validity of the blade element momentum theory. In *Proc. Eur. Wind Energy Conf. Exhib., Copenhagen*, pp. 362–66. Brussels: Eur. Wind Energy Assoc.

Sørensen JN, Myken A. 1992. Unsteady actuator disc model for horizontal axis wind turbines. *J. Wind Eng. Ind. Aerodyn.* 39:139–49

Sørensen JN, Shen WZ. 2002. Numerical modelling of wind turbine wakes. *J. Fluid Eng. Trans. ASME* 124:393–99

Sørensen JN, Shen WZ, Munduate X. 1998. Analysis of wake states by a full-field actuator disc model. *Wind Energy* 1:73–88

Sørensen JN, van Kuik GAM. 2010. General momentum theory for wind turbines at low tip speed ratios. *Wind Energy*. In press

Sørensen NN. 2009. CFD modelling of laminar-turbulent transition for airfoils and rotors using the $\gamma - \tilde{\mathrm{Re}}_{\theta}$ model. *Wind Energy* 12:715–33

Sørensen NN, Hansen MOL. 1998. *Rotor performance predictions using a Navier-Stokes method*. Presented at AIAA Aerosp. Sci. Meet. Exhib., 36th, Reno, AIAA Pap. No. 1998-25

Sørensen NN, Michelsen JA, Schreck S. 2002. Navier-Stokes predictions of the NREL phase VI rotor in the NASA-AMES 80 ft $\times$ 120 ft wind tunnel. *Wind Energy* 5:151–69

Spera DA. 1994. *Wind Turbine Technology*. New York: ASME

Stoddard FS. 1977. Momentum theory and flow states for windmill. *Wind Technol. J.* 1:3–9

Tangler JL. 2004. Insight into wind turbine stall and poststall aerodynamic. *Wind Energy* 7:247–60

Tangler JL, Somers DM. 1995. NREL airfoil families for HAWT's. In *Proc. WINDPOWER'95, Washington, DC*, pp. 117–23. Washington, DC: Am. Wind Energy Assoc.

Theodorsen T. 1948. *Theory of Propellers*. New York: McGraw-Hill

Tibery CL, Wrench JW. 1964. Tables of the Goldstein factor. David Taylor Model Basin. *Rep. 1534*, Appl. Math. Lab., Washington, DC

Timmer WA, van Rooij RPJOM. 1992. Thick airfoils for HAWT's. *J. Wind Eng. Ind. Aerodyn.* 39:151–60

Tongchitpakdec C, Benjanirat S, Sankar LN. 2005. *Recent improvements to a combined Navier-Stokes full potential methodology for modeling horizontal axis wind turbines*. Presented at AIAA Aerosp. Sci. Meet. Exhib., 43rd, Reno, AIAA Pap. No. 2005-773

Troldborg N. 2008. *Actuator line modelling of wind turbine wakes*. PhD diss. Dep. Mech. Eng., DTU, Lyngby, Denmark

Troldborg N, Sørensen JN, Mikkelsen R. 2010. Numerical simulations of wake characteristics of a wind turbine in uniform flow. *Wind Energy* 13:86–99

van Kuik GAM. 2007. The Lanchester-Betz-Joukowsky limit. *Wind Energy* 10:289–91

Veers P. 1988. Three-dimensional wind simulation. *Rep. SAND88–0152 UC-261*, Sandia Natl. Lab., Albuquerque

Verhoeff AJJ. 2005. *Aerodynamics of wind turbine rotors*. PhD thesis. Univ. Twente

Vermeer LJ. 2001. A review of wind turbine wake research at TU Delft. In *Proc. ASME Wind Energy Sympos. Tech. Pap.*, 103–13. New York: ASME

Vermeer LJ, Sørensen JN, Crespo A. 2003. Wind turbine wake aerodynamics. *Prog. Aerosp. Sci.* 39:467–510
Viterna LA, Corrigan RD. 1981. *Fixed-pitch rotor performance of large HAWT's*. Presented at DOE/NASA Workshop on Large HAWTs, Cleveland, Ohio
Voutsinas SG. 2006. Vortex methods in aeronautics: how to make things work. *Int. J. Comp. Fluid Dyn.* 20:3–18
Wald QR. 2006. The aerodynamics of propellers. *Prog. Aerosp. Sci.* 42:85–128
Whale J, Anderson CG, Bareiss R, Wagner S. 2000. An experimental and numerical study of the vortex structure in the wake of a wind turbine. *J. Wind Eng. Ind. Aerodyn.* 84:1–21
Wilson R, Lissaman PBS. 1974. *Applied Aerodynamics of Wind Power Machines*. Corvalis: Oregon State Univ.
Wilson RE, Lissaman PBS, Walker SN. 1976. Aerodynamic performance of wind turbines. *Rep. ERDA/NSF/04014-76/1*, Dep. Energy, Washington, DC
Wood DH. 2007. Including swirl in the actuator disck analysis of wind turbines. *Wind Eng.* 31:317–23
Wussow S, Sitzki L, Hahm T. 2007. 3D simulation of the turbulent wake behind a wind turbine. *J. Phys. Conf. Ser.* 75:012033
Xiros MI, Xiros NI. 2007. Remarks on wind turbine power absorption increase by including the axial force due to the radial pressure gradient in the general momentum theory. *Wind Energy* 10:99–102
Xu G, Sankar LN. 2000. Computational study of horizontal axis wind turbines. *J. Sol. Energy Eng.* 122:35–39
Xudong W, Shen WZ, Zhu WJ, Sørensen JN, Jin C. 2009. Shape optimization of wind turbine blades. *Wind Energy* 12:781–803
Zahle F, Sørensen NN, Johansen J. 2009. Wind turbine rotor-tower interaction using an incompressible overset grid method. *Wind Energy* 12:594–619

RELATED RESOURCES

Burton T, Sharpe D, Jenkins N, Bossanyi E. 2001. *Wind Energy Handbook*. New York: Wiley.
Hansen AC, Butterfield CP. 1993. Aerodynamics of horizontal-axis wind turbines. *Annu. Rev. Fluid Mech.* 25:115–49
Hansen MOL. 2008. *Aerodynamics of Wind Turbine*. London: Earthscan
Hansen MOL, Sørensen JN, Voutsinas S, Sørensen N, Madsen HA. 2006. State of the art in wind turbine aerodynamics and aeroelasticity. *Prog. Aerosp. Sci.* 42:285–330
Leishman JG. 2002. Challenges in modeling the unsteady aerodynamics of wind turbines. *Wind Energy* 5:86–132
Snel H. 1998. Review of the present status of rotor aerodynamics. *Wind Energy* 1:46–69

Annual Review of
Fluid Mechanics

Volume 43, 2011

Contents

Experimental Studies of Transition to Turbulence in a Pipe
T. Mullin 1

Fish Swimming and Bird/Insect Flight
Theodore Yaotsu Wu 25

Wave Turbulence
Alan C. Newell and Benno Rumpf 59

Transition and Stability of High-Speed Boundary Layers
Alexander Fedorov 79

Fluctuations and Instability in Sedimentation
Élisabeth Guazzelli and John Hinch 97

Shock-Bubble Interactions
Devesh Ranjan, Jason Oakley, and Riccardo Bonazza 117

Fluid-Structure Interaction in Internal Physiological Flows
Matthias Heil and Andrew L. Hazel 141

Numerical Methods for High-Speed Flows
Sergio Pirozzoli 163

Fluid Mechanics of Papermaking
Fredrik Lundell, L. Daniel Söderberg, and P. Henrik Alfredsson 195

Lagrangian Dynamics and Models of the Velocity Gradient Tensor in Turbulent Flows
Charles Meneveau 219

Actuators for Active Flow Control
Louis N. Cattafesta III and Mark Sheplak 247

Fluid Dynamics of Dissolved Polymer Molecules in Confined Geometries
Michael D. Graham 273

Discrete Conservation Properties of Unstructured Mesh Schemes
J. Blair Perot 299

Global Linear Instability
Vassilios Theofilis 319

High–Reynolds Number Wall Turbulence
Alexander J. Smits, Beverley J. McKeon, and Ivan Marusic 353

Scale Interactions in Magnetohydrodynamic Turbulence
Pablo D. Mininni 377

Optical Particle Characterization in Flows
Cameron Tropea 399

Aerodynamic Aspects of Wind Energy Conversion
Jens Nørkær Sørensen 427

Flapping and Bending Bodies Interacting with Fluid Flows
Michael J. Shelley and Jun Zhang 449

Pulse Wave Propagation in the Arterial Tree
Frans N. van de Vosse and Nikos Stergiopulos 467

Mammalian Sperm Motility: Observation and Theory
E.A. Gaffney, H. Gadêlha, D.J. Smith, J.R. Blake, and J.C. Kirkman-Brown 501

Shear-Layer Instabilities: Particle Image Velocimetry Measurements and Implications for Acoustics
Scott C. Morris 529

Rip Currents
Robert A. Dalrymple, Jamie H. MacMahan, Ad J.H.M. Reniers, and Varjola Nelko 551

Planetary Magnetic Fields and Fluid Dynamos
Chris A. Jones 583

Surfactant Effects on Bubble Motion and Bubbly Flows
Shu Takagi and Yoichiro Matsumoto 615

Collective Hydrodynamics of Swimming Microorganisms: Living Fluids
Donald L. Koch and Ganesh Subramanian 637

Aerobreakup of Newtonian and Viscoelastic Liquids
T.G. Theofanous 661

Indexes

Cumulative Index of Contributing Authors, Volumes 1–43 691

Cumulative Index of Chapter Titles, Volumes 1–43 699

Errata

An online log of corrections to *Annual Review of Fluid Mechanics* articles may be found at http://fluid.annualreviews.org/errata.shtml